Effect of quenching medium on photocatalytic activity of nano-TiO$_2$ prepared by solvothermal method

Piyawat Supphasrirongjaroen [a], Piyasan Praserthdam [a,*], Joongjai Panpranot [a],
Duangkamol Na-Ranong [b], Okorn Mekasuwandumrong [c]

[a] *Center of Excellence on Catalysis and Catalytic Reaction Engineering, Department of Chemical Engineering,
Faculty of Engineering, Chulalongkorn University, Bangkok 10330, Thailand*
[b] *Department of Chemical Engineering, Faculty of Engineering,
King Mongkut's Institute of Technology Ladkrabang, Bangkok 10520, Thailand*
[c] *Department of Chemical Engineering, Faculty of Engineering and Industrial Technology,
Silpakorn University, Nakhonphatom 73000, Thailand*

Abstract

Pure anatase nano-TiO$_2$ powders were synthesized by solvothermal method using titanium butoxide as the precursor and were subjected to a rapid quenching in various media such as H$_2$O, H$_2$O$_2$, air, and liquid N$_2$ as a post-synthesis treatment. By creating a thermal shock effect, quenching process has shown to be an easy novel route for modifying surface defects of the nano-TiO$_2$ and its photocatalytic activity. In this study, the TiO$_2$ sample quenched in air at 77 K contained the highest amount of Ti^{3+} surface defect with the highest Ti^{3+}/OH and was found to exhibit the highest photocatalytic activity for ethylene decomposition.
© 2007 Elsevier B.V. All rights reserved.

Keywords: Titanium dioxide; TiO$_2$; Photocatalyst; Solvothermal; Ethylene decomposition; Quenching; Defects

1. Introduction

Nanoparticle TiO$_2$ semiconductor is a very useful material and has been employed in various fields such as solar cells, photocatalytic splitting of water for green-energy hydrogen production, selective synthesis of organic compounds, air purification, removal of organic and inorganic pollutants, and photokilling of pathogenic organisms [1–4]. In general, when TiO$_2$ nanoparticles adsorb light (wavelength smaller than 385 nm), the valence band electron jumps through the band gap to the conduction band, leaving a positive hole in valence band, and generating an electron–hole pair. These pairs are able to initiate redox reactions to destroy the organic species adsorbed on the TiO$_2$ surfaces. The photocatalytic activity of TiO$_2$ strongly depends on preparation methods and post-treatment conditions since they have a decisive influence on crystal phase and size,

specific surface area, pore–wall structure, as well as the surface properties, particularly surface defect, of the TiO$_2$ [5,6].

Various techniques have been reported for the preparation of nano-TiO$_2$ such as solvothermal method [7–10], precipitation method [11], sol–gel method [12–14], chemical vapor deposition [15], and thermal decomposition of alkoxide [16]. The sol–gel method is an easy method but the precipitated powders obtained are amorphous in nature and further heat treatment is required for crystallization. Solvothermal method is an alternative route for direct (one-step) synthesis of pure anatase nano-TiO$_2$. Particle morphology, crystalline phase, and surface chemistry of the solvothermal-derived TiO$_2$ can be controlled by regulating precursor composition, reaction temperature, pressure, solvent property, and aging time.

In order to improve the photocatalytic activity of TiO$_2$ under UV light region, different methods have been studied such as ion implantation [17], doping with transition metals [18,19], the use of two semiconductors composite [20], sulfation [21,22], reduction with hydrogen [23], halogenation, [24] and the creation of surface defect [25]. However, most of the improvement meth-

* Corresponding author. Tel.: +66 2 218 6766; fax: +66 2 218 6769.
 E-mail address: piyasan.p@chula.ac.th (P. Praserthdam).

ods reported in the literature are time-consuming, high cost, and rather complicated.

In this study, quenching process has been applied as a post-synthesis treatment for enhancement of photocatalytic activity of nano-TiO$_2$ synthesized by solvothermal method. Quenching is defined as the mechanism of "rapid cooling" of material (cooling from a relatively high temperature to a fairly low temperature in a short period of time). The process of annealing or quenching has shown to result in a variety of surface defects, strains, and reconstructions of materials [26]. The effects of quenching medium (liquid N$_2$, H$_2$O, H$_2$O$_2$, and air) and quenching temperature on physicochemical properties of the nano-TiO$_2$ synthesized by solvothermal method were investigated in details using X-ray diffraction (XRD), X-ray photoelectron spectroscopy (XPS), N$_2$ physisorption, and CO$_2$ temperature programmed desorption. The photocatalytic activity of the TiO$_2$ nanoparticles was evaluated in the gas-phase decomposition of ethylene under UV irradiation.

2. Experimental

2.1. Preparation of nano-TiO$_2$

Nanocrystalline TiO$_2$ was prepared using the solvothermal method in the same manner as that of Payakgul et al. [27]. Titanium(IV) *n*-butoxide (purity 97%, Aldrich) was used as the starting material. Approximately 25 g of titanium *n*-butoxide was suspended in 100 ml of toluene, in a test tube, which was then placed in a 300 ml autoclave. The same solvent was filled in the gap between the test tube and the autoclave wall. The autoclave was purged completely by nitrogen after that it was heated up to the desired temperature at 573 K with the rate of 2.5 K/min. The temperature of the autoclave was held constant at 573 K for 2 h and then cooled down to room temperature. The obtained TiO$_2$ was washed by methanol for several times and finally dried in air.

2.2. Quenching treatment

Prior to quenching, the synthesized TiO$_2$ was dried in air atmosphere at 573 K with a heating rate of 10 K/min for 1 h and then it was taken out and immediately quenched in various quenching media. In this study, both liquid phase and gas-phase media were used. For quenching in liquid phase media, liquid nitrogen at 77 K (sample A), water at room temperature and 373 K (samples B and C), and hydrogen peroxide (30% wt, Merck) at room temperature and 373 K (samples D and E) were selected. For quenching in gas-phase media, air at room temperature and 77 K (samples F and G) were used. After the samples were quenched in selected media for 30 min, all samples were dried in air at room temperature and stored in a desiccator.

2.3. Catalyst characterization

The Brunauer–Emmett–Teller (BET) surface area (S_{BET}) was determined by nitrogen adsorption at 77 K in a Micromeritics Chemisorb 2750 automated system. All the samples were dried at 150 °C for 30 min in a 30% N$_2$-helium flow prior to measurements. The X-ray diffraction (XRD) patterns of TiO$_2$ were recorded with an X-ray diffractometer (SIEMENS, D-5000) using Cu Kα radiation with a Ni filter in the 2θ range from 20° to 80° with a scanning rate of 0.04°/min. The powder was contained in a flat holder. The average anatase crystallite diameter $d_{Scherrer}$ was determined from half-height width of the 1 0 1 diffraction peak of anatase using the Scherrer equation. Temperature programmed desorption using CO$_2$ as a probe molecule (CO$_2$-TPD) was performed in order to determine the Ti^{3+} defective sites existing on the surface of TiO$_2$ particle [28]. Approximately 0.05 g of a TiO$_2$ sample was dosed by 1 vol.% CO$_2$ in helium for 1 h and then desorbed from 143 to 273 K with the rate of 21.5 K/min. The XPS measurement was carried out using an AMICUS photoelectron spectrometer equipped with an Mg Kα X-ray as a primary excitation and KRATOS VISION2 software. XPS elemental spectra were acquired with 0.1 eV energy step at a pass energy of 75 kV. All the binding energies were referenced to the C 1s peak at 285 eV of the surface adventitious carbon. TEM images were obtained using the JEOL JEM 2010 transmission electron microscope that employed a LaB$_6$ electron gun in the voltage range of 80–200 kV with an optical point to point resolution of 0.23 nm.

2.4. Photocatalytic activity measurement

Photocatalytic decomposition of ethylene (C$_2$H$_4$) was used to as a model reaction to examine the photocatalytic activity of the synthesized TiO$_2$. Ethylene is harmful to all like forms, in order to keep enough food fresh in the CELSS (Controlled Ecological Life Support Systems), it is necessary to remove ethylene, which is released from plants. The complete photocatalytic oxidation of ethylene with oxygen into carbon dioxide and water has been achieved on ultrafine powdered TiO$_2$ photocatalysts [29]. All the experiments were carried out using horizontal quartz fixed bed reactor (i.d. 9 mm, length 60 cm). The weight of the catalyst was kept constant at 0.4 g. In order to avoid light penetration from outside, the reactor was placed in a closed stainless box at top of which a 500 W mercury lamp (Philips, HPL-N) was provided, emitting in the UV light region. Before exposure to the pollutant of interest, the photocatalyst sample is briefly cleaned by simultaneous exposure to UV and flowing air for 60 min [30]. Then, high purity grade air containing 0.1 vol.% ethylene was continuously fed at a constant flow rate with GHSV of 120 h^{-1}. The outlet gas was sampled every 30 min. Product compositions were analyzed using a SHIMADZU GC-14B gas chromatograph equipped with the flame ionized detector and a VZ-10 column, until the reaction reached steady-state.

3. Results and discussion

3.1. Characteristics of the nano-sized TiO$_2$

The properties of the solvothermal-derived nano-TiO$_2$ quenched in different media are given in Table 1. As shown by XRD results, all the nano-TiO$_2$ samples prepared by the solvothermal method in this study were anatase phase TiO$_2$ with

Table 1
Effects of quenching treatment on the physical properties and activities of TiO_2 samples synthesized by solvothermal method

Sample	Quenching medium	Crystallite size[a] (nm)	Specific surface area[b] (m^2/g)	Surface Ti^{3+}[c] (%)	Surface OH[c] (%)	Ratio Ti^{3+}/OH	Ethylene conversion[d] (%)
A	Liquid N_2	11	87	7.86	10.91	0.72	24.5
B	H_2O at RT	10	112	8.67	10.96	0.79	27.8
C	H_2O at 373 K	11	94	8.09	10.46	0.77	26.0
D	30% wt H_2O_2 at RT	13	94	8.88	9.79	0.91	32.5
E	30% wt H_2O_2 at 373 K	13	90	8.83	10.31	0.86	31.8
F	Air at RT	11	93	7.40	10.43	0.71	21.6
G	Air at 77 K	11	97	9.35	10.06	0.93	34.6

[a] Determined using Scherrer's equation (applicable from 3 to 200 nm).
[b] Determined using BET method.
[c] Determined using XPS.
[d] Photocatalytic reaction was carried out at 313–328 K, 1 bar, and 0.1% ethylene in air.

average crystallite size determined from the half-width of peaks using Scherrer's formula ($d = 0.9\lambda/\beta \cos\theta$) around 10–13 nm. The XRD patterns of the TiO_2 samples quenched in different media (air, hydrogen peroxide, water, and liquid N_2 at different temperatures) were not significantly different (Fig. 1); only the characteristic peaks of pure anatase phase TiO_2 were observed at $2\theta = 25.36°, 37.82°, 48.18°$ [31]. The specific surface areas of the TiO_2 samples were found to be 87–112 m^2/g.

Fig. 2 shows transmission electron micrographs (TEM) and high resolution electron micrographs (HRTEM) for the as-prepared TiO_2 powders. The as-prepared powders consist of crystalline particles with primarily spheroidal shape with the size around 8–15 nm. The crystallite size calculated by Scherrer equation (11 nm) was in good agreement with size of the primary particle observed by TEM. It is revealed that each primary particle was a single crystal TiO_2.

The characteristics of surface adsorption sites of the TiO_2 samples were studied by means of temperature program desorption of CO_2 from 143 to 273 K. The results are shown in Fig. 3. All of the TiO_2 samples exhhibited two main desorption peaks at 170 and 200 K which can be assigned to CO_2 molecules bonded to different adsorption sites on the surface. The first peak at ca. 170 K was assigned to Ti^{4+} sites (perfect TiO_2 structure) and the second one at 200 K was assigned to Ti^{3+} sites or defect TiO_2 structure [28]. The amounts of surface Ti^{3+}
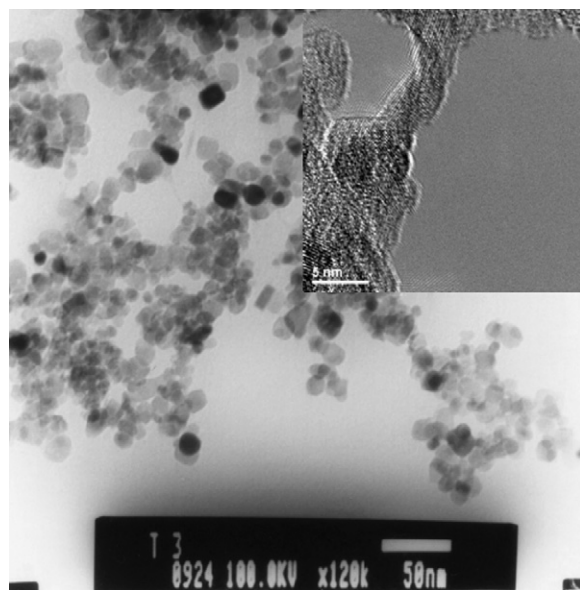

Fig. 2. TEM images of as-prepared TiO_2.

sites on the TiO_2 samples were observed from the areas under the Ti^{3+} TPD peaks and were found to be in the following order: air at 77 K > 30% H_2O_2 at RT > 30% H_2O_2 at 373 K > H_2O at RT > H_2O at 373 K > liquid N_2 > air at RT.

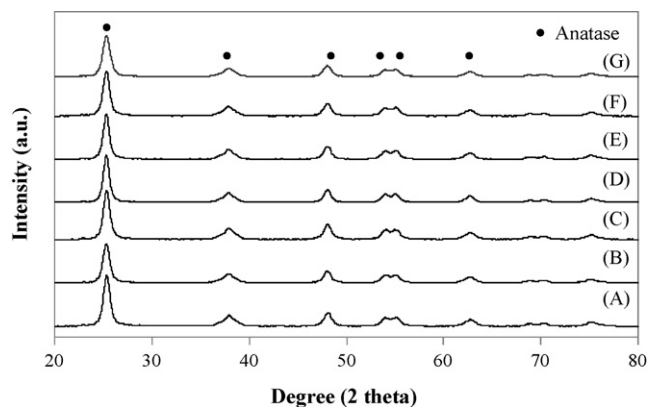

Fig. 1. The XRD patterns of the TiO_2 obtained from quenching in various media: (A) liquid N_2, (B) H_2O at RT, (C) H_2O at 373 K, (D) 30% H_2O_2 at RT, (E) 30% H_2O_2 at 373 K, (F) air at RT, and (G) air at 77 K.
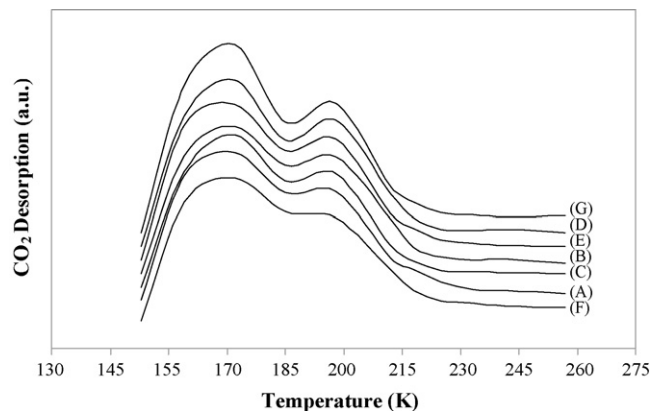

Fig. 3. Thermal desorption spectra for CO_2 adsorbed on TiO_2 quenched in different media: (A) liquid N_2, (B) H_2O at RT, (C) H_2O at 373 K, (D) 30% H_2O_2 at RT, (E) 30% H_2O_2 at 373 K (F) air at RT, and (G) air at 77 K.
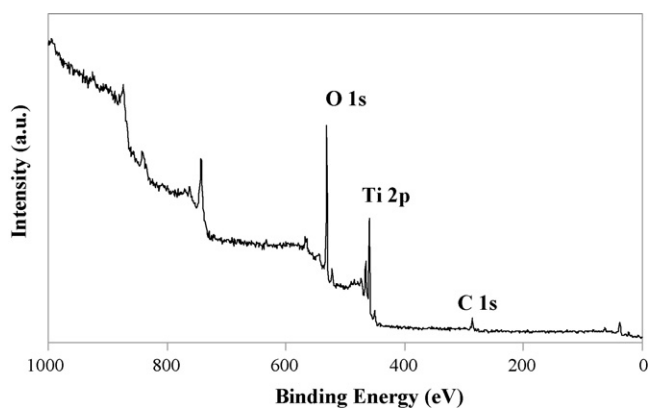
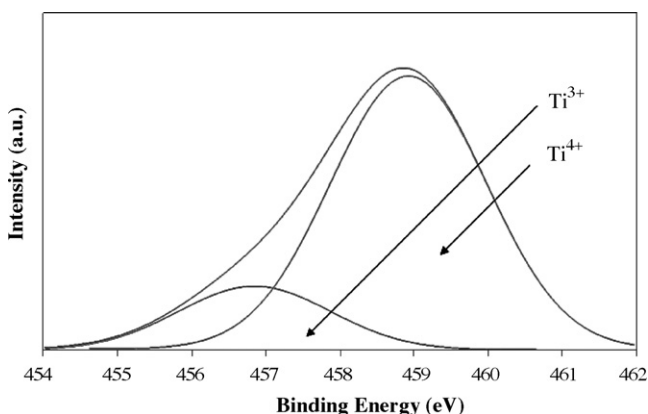Fig. 4. Overview X-ray photoelectron spectra in the case of TiO₂ sample quenched in 30% hydrogen peroxide at room temperature.

Fig. 6. O 1s XPS spectra for TiO₂ sample quenched in 30% wt hydrogen peroxide at room temperature.

The elements and their chemical states on surface of the TiO₂ samples after quenching treatment were also studied by XPS analysis. The typical XPS survey spectra of the TiO₂ powders after quenching treatment indicated that the powder was mainly composed of Ti and O elements with a small amount of C element (Fig. 4). The shapes of the XPS spectra of Ti 2p and O 1s for all the TiO₂ samples are quite similar. For example, the high-resolution XPS spectra of Ti 2p recorded from the TiO₂ samples quenched in H_2O_2 at room temperature are shown in Fig. 5. The Ti 2p spectrum can be fitted with Gaussian–Lorentzian functions into two spin–orbit components at binding energies 457.2 and 459.2 eV corresponding to Ti_2O_3 (Ti^{3+}) and TiO_2 (Ti^{4+}) fractions on the TiO₂ surface, respectively. The component binding energy values are in agreement with those reported in the literature [32]. The XPS O 1s spectra of the TiO₂ sample quenched in hydrogen peroxide at room temperature is also presented in Fig. 6. The O 1s peak is often believed to be composed of 3–5 different oxygen species such as Ti–O bonds in TiO₂ and Ti_2O_3, hydroxyl groups, C–O bonds, and adsorbed H_2O. It is shown that the O 1s peak is asymmetric suggesting that at least three peaks related to three different chemical states of oxygen are present. The binding energies of each individual components are 530.8 (Ti^{4+}–O), 531.8 (Ti^{3+}–O), and 533.3 eV (O–H) [33,34]. It was found that the amount of surface Ti^{3+} sites increased in a sim-

ilar trend as those observed from CO_2-TPD results. The TiO₂ quenched in different media thus possessed different surface properties especially in terms of the amount of Ti^{3+} defect sites on TiO₂ surface.

3.2. Photocatalytic activity of the nano-TiO₂ quenched in different media

Photocatalytic decomposition of ethylene was conducted to assess the photocatalytic activity of the TiO₂ samples quenched in various media. The amounts of adsorbed ethylene on the catalyst surface before degradation experiments were quite similar among the various catalysts as confirmed by ethylene-chemisorption and temperature programmed desorption experiments (results not shown). The plots of ethylene conversion as a function of reaction time for all the samples are shown in Fig. 7. Photocatalytic activity of the nano-sized TiO₂ quenched in different media is evidently different. The mechanism of photocatalytic decomposition of ethylene was reported by many researchers [35,36]. Yamazaki et al. [35] proposed the reaction sequences based on Langmuir–Hinshelwood model as follows:

$$C_2H_4 + \sigma \rightarrow C_2H_4\sigma \tag{1}$$

$$H_2O + \sigma \rightarrow H_2O\sigma \tag{2}$$

Fig. 5. Ti 2p XPS spectra for TiO₂ sample quenched in 30% wt hydrogen peroxide at room temperature.

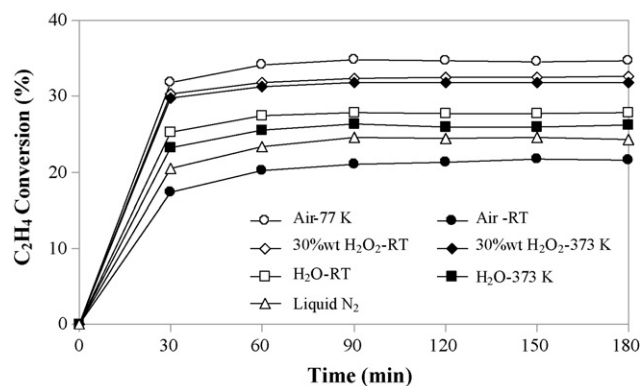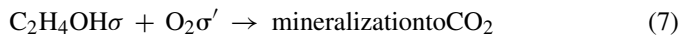Fig. 7. Results of photocatalytic testing comparing the activities of different TiO₂ samples.

$$O_2 + \sigma' \rightarrow O_2\sigma' \tag{3}$$

$$TiO_2 + h\nu \rightarrow h^+(VB) + e^-(CB) \tag{4}$$

$$H_2O\sigma + h^+(VB) \rightarrow OH\sigma + H^+\sigma \tag{5}$$

$$OH\sigma + C_2H_4\sigma \rightarrow C_2H_4OH\sigma \tag{6}$$

$$C_2H_4OH\sigma + O_2\sigma' \rightarrow mineralization\ to\ CO_2 \tag{7}$$
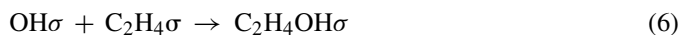
where σ and σ' mean different types of active sites on the TiO$_2$ surface. From reaction mechanism mentioned above, the hole generated from photo-excitation process plays an important role on creating the reaction intermediate, which react further and form CO$_2$ as the final product.

From early characterization results (XPS and CO$_2$-TPD), it is likely that quenching process can modify surface properties of the TiO$_2$ samples, i.e., enhancing the amount of surface defects (Ti^{3+}) so that higher photocatalytic activity was obtained. The relationship between the amount of Ti^{3+} surface defect on the TiO$_2$ samples quenched in different media and ethylene conversion is illustrated in Fig. 8. The surface Ti^{3+} defect sites on TiO$_2$ photocatalysts has been found to play an important role determining their photocatalytic activity since they can act as photoelectron trapping sites [19,29].

In photocatalysis, light irradiation of TiO$_2$ powder with a photon energy larger than the band-gap energy produces electrons (e$^-$) and holes (h$^+$) in the conduction band and the valence band, respectively. These electrons and holes are thought to have the respective abilities to reduce and oxidize chemical species adsorbed on the surface of TiO$_2$ particles. For a photocatalyst to be most efficient, different interfacial electron processes involving e$^-$ and h$^+$ must compete effectively with the major deactivation processes involving e$^-$–h$^+$ recombination. Park et al. [29] has reported that modification of TiO$_2$ surface by increasing the amount of Ti^{3+} surface defects can increase the photocatalytic activity of TiO$_2$. It is suggested that the photoelectrons were trapped by the surface defect (Ti^{3+}) leading to inhibition of the e$^-$–h$^+$ recombination. In addition, Yu et al. [19] proposed that the doped F atoms convert Ti^{4+} to Ti^{3+} by

charge compensation and that the presence of a certain amount of Ti^{3+} reduces the electron–hole recombination rate and thus enhances the photocatalytic activity.

Recently, Chen et al. [37] reported that the trapping site of photogenerated holes or the surface OH is also an important factor affecting photo-catalytic reaction besides the surface Ti^{3+}. The nano-crystalline TiO$_2$ particles showed better photocatalytic activities when Ti^{3+}/OH ratios on the TiO$_2$ surface were close to 1. In this study, Ti^{3+}/OH ratios of the nano-TiO$_2$ quenched in various media were calculated based on the XPS results and are given in Table 1. It was also found that the TiO$_2$ quenched in air at 77 K (sample G) with Ti^{3+}/OH ratio = 0.93 (closest to 1 among the various samples) exhibited the highest photocatalytic activity. Thus, it is clearly shown from this study that quenching condition and medium during post-synthesis treatment strongly affect photocatalytic activity of the nano-TiO$_2$. Considering the TiO$_2$ samples quenched in the same type of quenching media (i.e., in H$_2$O, 30% H$_2$O$_2$, or air), it was found that TiO$_2$ samples quenched at lower temperature exhibited higher photocatalytic activity than those quenched in high temperature ones. For example, TiO$_2$ quenched in air at 77 K showed higher ethylene conversion than the one quenched in air at room temperature. These results can probably be explained in terms of the thermal shock effect. The large difference in temperature between media and TiO$_2$ surface may lead to modification of the surface properties, i.e., increasing the amount of Ti^{3+} defects on the TiO$_2$ surface. Additionally, it is noted that for the used of liquid phase media, the TiO$_2$ sample quenched in the media containing more –OH group in molecules exhibited higher photocatalytic activity.

4. Conclusions

In this study, we have shown that surface properties as well as photocatalytic activities of the solvothermal-derived nano-TiO$_2$ can be modified by quenching process post-synthesis treatment whilst the average crystallite size and BET surface area of the samples were essentially similar. It was found that quenching process especially the use of low temperature medium can create a thermal shock effect that as a consequence resulting in more surface Ti^{3+} defects on the TiO$_2$ sample and hence higher photocatalytic activity.

References

[1] A.L. Linsebigler, G. Lu, J.T. Yates Jr., Photocatalysis on TiO$_2$ surfaces: principles, mechanisms, and selected results, Chem. Rev. 95 (1995) 735–758.
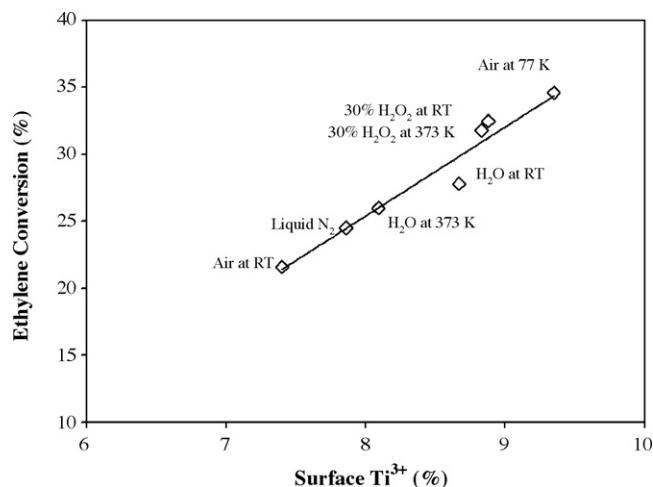

Fig. 8. Ethylene conversions as a function of surface Ti^{3+} on the TiO$_2$ samples quenched in different media.

[2] O. Carp, C.L. Huisman, A. Reller, Photoinduced reactivity of titanium dioxide, Prog. Solid State Chem. 32 (2004) 33–177.

[3] V.N.H. Nguyen, R. Amal, D. Beydoun, Effect of formate and methanol on photoreduction/removal of toxic cadmium ions using TiO₂ semiconductor as photocatalyst, Chem. Eng. Sci. 58 (2003) 4429–4439.

[4] D. Chen, A.K. Ray, Removal of toxic metal ions from wastewater by semiconductor photocatalysis, Chem. Eng. Sci. 56 (2001) 1561–1570.

[5] J. Yu, X. Zhao, J. Du, W. Chen, Preparation, microstructure and photocatalytic activity of the porous TiO₂ anatase coating by sol–gel processing, J. Sol–Gel Sci. Technol. 17 (2000) 163–171.

[6] J.-G. Yu, H.-G. Yu, B. Cheng, X.-J. Zhao, J.C. Yu, W.-K. Ho, The effect of calcination temperature on the surface microstructure and photocatalytic activity of TiO₂ thin films prepared by liquid phase deposition, J. Phys. Chem. B 107 (2003) 13871–13879.

[7] C.-S. Kim, B.K. Moon, J.-H. Park, S.T. Chung, S.-M. Son, Synthesis of nanocrystalline TiO₂ in toluene by a solvothermal route, J. Cryst. Growth 254 (2003) 405–410.

[8] C. Wang, Z.-X. Deng, G. Zhang, S. Fan, Y. Li, Synthesis of nanocrystalline TiO₂ in alcohols, Powder Technol. 125 (2002) 39–44.

[9] M. Kang, B.-J. Kim, S.M. Cho, C.-H. Chung, B.-W. Kim, G.Y. Han, K.J. Yoon, Decomposition of toluene using an atmospheric pressure plasma/TiO₂ catalytic system, J. Mol. Catal. A: Chem. 180 (2002) 125–132.

[10] H. Kominami, M. Kohno, Y. Takada, M. Inoue, T. Inui, Y. Kera, Hydrolysis of titanium alkoxide in organic solvent at high temperatures: a new synthetic method for nanosized, thermally stable titanium(IV) oxide, Ind. Eng. Chem. Res. 38 (1999) 3925–3931.

[11] H.-D. Nam, B.-H. Lee, S.-J. Kim, C.-H. Jung, J.-H. Lee, S. Park, Preparation of ultrafine crystalline TiO₂ powders from aqueous TiCl₄ solution by precipitation, Jpn. J. Appl. Phys. 37 (1998) 4603–4608.

[12] C. Su, B.-Y. Hong, C.-M. Tseng, Sol–gel preparation and photocatalysis of titanium dioxide, Catal. Today 96 (2004) 119–126.

[13] P. Yang, C. Lu, N. Hua, Y. Du, Titanium dioxide nanoparticles co-doped with Fe³⁺ and Eu³⁺ ions for photocatalysis, Mater. Lett. 57 (2002) 794–801.

[14] Y. Bessekhouad, D. Robert, J.V. Weber, Synthesis of photocatalytic TiO₂ nanoparticles: optimization of the preparation conditions, J. Photochem. Photobiol. A: Chem. 157 (2003) 47–53.

[15] K. Nakaso, K. Okuyama, M. Shimada, S.E. Pratsinis, Effect of reaction temperature on CVD-made TiO₂ primary particle diameter, Chem. Eng. Sci. 58 (2003) 3327–3335.

[16] H. Kominami, J.-I. Kalo, Y. Takada, Y. Doushi, B. Ohtani, S.-I. Nishimoto, M. Inoue, T. Inui, Y. Kera, Novel synthesis of microcrystalline titanium(IV) oxide having high thermal stability and ultra-high photocatalytic activity: thermal decomposition of titanium(IV) alkoxide in organic solvents, Catal. Lett. 46 (1997) 235–240.

[17] T. Umebayashi, T. Yamaki, S. Yamamoto, A. Miyashita, S. Tanaka, T. Sumita, K. Asai, Sulfur-doping of rutile-titanium dioxide by ion implantation: photocurrent spectroscopy and first-principles band calculation studies, J. Appl. Phys. 93 (2003) 5156–5160.

[18] M. Anpo, M. Takeuchi, The design and development of highly reactive titanium oxide photocatalysts operating under visible light irradiation, J. Catal. 216 (2003) 505–516.

[19] J.C. Yu, J. Yu, W. Ho, Z. Jiang, L. Zhang, Effects of F-doping on the photocatalytic activity and microstructures of nanocrystalline TiO₂ powders, Chem. Mater. 14 (2002) 3808–3816.

[20] D. Li, H. Haneda, Photocatalysis of sprayed nitrogen-containing Fe₂O₃-ZnO and WO₃-ZnO composite powders in gas-phase acetaldehyde decomposition, J. Photochem. Photobiol. A 160 (2003) 203–212.

[21] A. Corma, A. Martínez, C. Martínez, The effect of sulfation conditions and activation temperature of sulfate-doped ZrO₂, TiO₂ and SnO₂ catalysts during isobutane/2-butene alkylation, Appl. Catal. A: Gen. 144 (1996) 249–268.

[22] E. Barraud, F. Bosc, D. Edwards, N. Keller, V. Keller, Gas phase photocatalytic removal of toluene effluents on sulfated titania, J. Catal. 235 (2005) 318–326.

[23] H. Liu, H.T. Ma, X.Z. Li, W.Z. Li, M. Wu, X.H. Bao, The enhancement of TiO₂ photocatalytic activity by hydrogen thermal treatment, Chemosphere 50 (2003) 39–46.

[24] P.B. Amama, K. Itoh, M. Murabayashi, Gas-phase photocatalytic degradation of trichloroethylene on pretreated TiO₂, Appl. Catal. B: Environ. 37 (2002) 321–330.

[25] I. Nakamura, N. Negishi, S. Kutsuna, T. Ihara, S. Sugihara, K. Takeuchi, Role of oxygen vacancy in the plasma-treated TiO₂ photocatalyst with visible light activity for NO removal, J. Mol. Catal. A 161 (2000) 205–212.

[26] M.A. Henderson, An HREELS and TPD study of water on TiO₂(1 1 0): the extent of molecular versus dissociative adsorption, Surf. Sci. 355 (1996) 151–166.

[27] W. Payakgul, O. Mekasuwandumrong, V. Pavarajarn, P. Praserthdam, Effects of reaction medium on the synthesis of TiO₂ nanocrystals by thermal decomposition of titanium(IV) n-butoxide, Ceram. Int. 31 (2005) 391–397.

[28] T.L. Thompson, O. Diwald, J.T. Yates Jr., CO₂ as a probe for monitoring the surface defects on TiO₂(1 1 0)-temperature-programmed desorption, J. Phys. Chem. B 107 (2003) 11700–11704.

[29] D.-R. Park, J. Zhang, K. Ikeue, H. Yamashita, M. Anpo, Photocatalytic oxidation of ethylene to CO₂ and H₂O on ultrafine powdered TiO₂ photocatalysts in the presence of O₂ and H₂O, J. Catal. 185 (1999) 114–119.

[30] M. Lewandowski, D.F. Ollis, Halide acid pretreatments of photocatalysts for oxidation of aromatic air contaminants: rate enhancement, rate inhibition, and a thermodynamic rationale, J. Catal. 217 (2003) 38–46.

[31] S.S. Watson, D. Beydoun, J.A. Scott, R. Amal, The effect of preparation method on the photoactivity of crystalline titanium dioxide particles, Chem. Eng. J. 95 (2003) 213–220.

[32] P.M. Kumar, S. Badrinarayanan, M. Sastry, Nanocrystalline TiO₂ studied by optical, FTIR and X-ray photoelectron spectroscopy: correlation to presence of surface states, Thin Solid Films 358 (2000) 122–130.

[33] J. Yu, X. Zhao, Q. Zhao, Effect of surface structure on photocatalytic activity of TiO₂ thin films prepared by sol–gel method, Thin Solid Films 379 (2000) 7–14.

[34] J. Pouilleau, D. Devilliers, H. Groult, P. Marcus, Surface study of a titanium-based ceramic electrode material by X-ray photoelectron spectroscopy, J. Mater. Sci. 32 (1997) 5645–5651.

[35] S. Yamazaki, S. Tanaka, H. Tsukamoto, Kinetic studies of oxidation of ethylene over a TiO₂ photocatalyst, J. Photochem. Photobiol. A: Chem. 121 (1999) 55–61.

[36] A. Sirisuk, C.G. Hill, M.A. Anderson, Photocatalytic degradation of ethylene over thin films of titania supported on glass rings, Catal. Today 54 (1999) 159–164.

[37] X.-Q. Chen, H.-B. Liu, G.-B. Gu, Preparation of nanometer crystalline TiO₂ with high photo-catalytic activity by pyrolysis of titanyl organic compounds and photo-catalytic mechanism, Mater. Chem. Phys. 91 (2005) 317–324.